

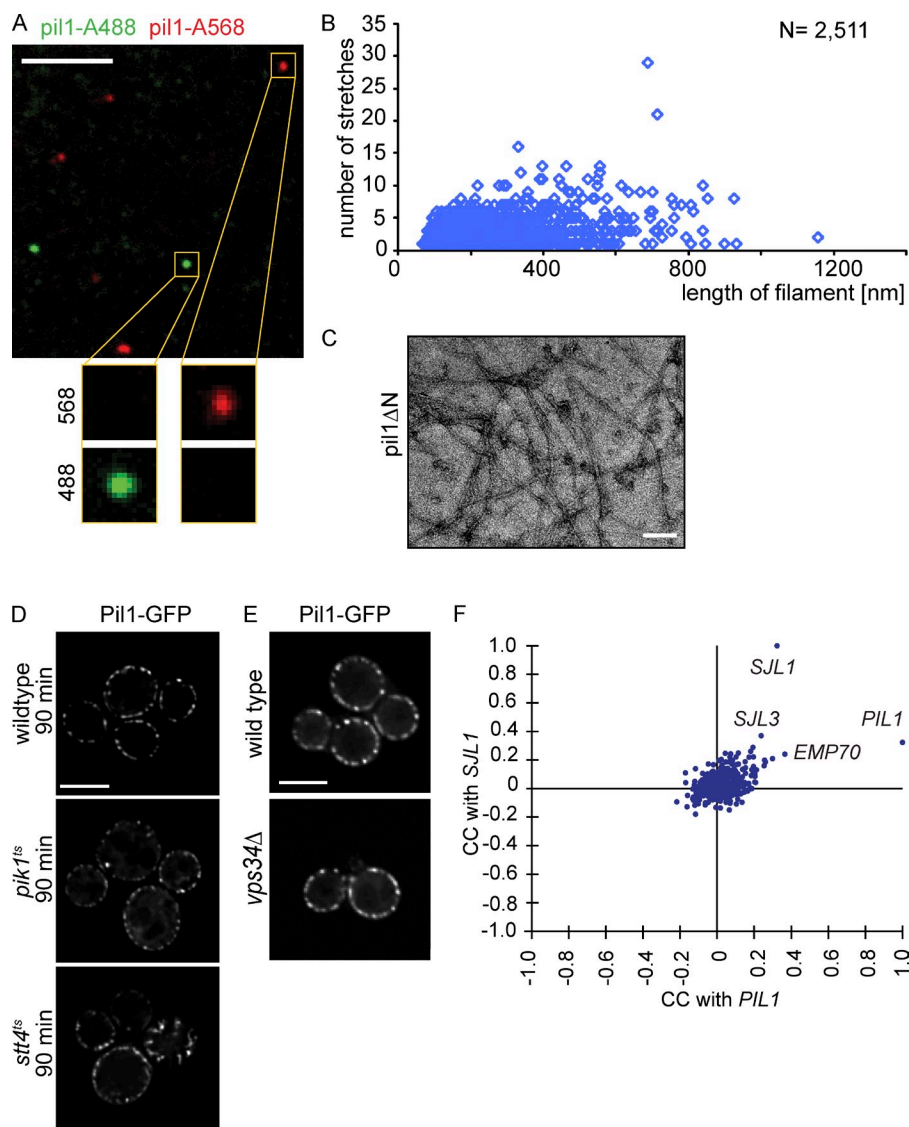
Karotki et al., <http://www.jcb.org/cgi/content/full/jcb.201104040/DC1>

Figure S1. **Eisosome proteins form highly stable filaments of variable diameter, and their localization is specifically dependent on plasma membrane PI(4,5)P<sub>2</sub>.** (A) Recombinant Pil1 was mutated by single-amino acid replacement to pil1 (A254C) and coupled to either an Alexa Fluor 488 (denoted pil1-A488) or 568 (denoted pil1-A568) fluorophore, incubated for 3 h, and imaged by fluorescence microscopy. Mutation and labeling had no influence on localization of Pil1 or Lsp1 in eisosomes or the assembly in vitro or in vivo, respectively (not depicted). Recombinant labeled pil1 (A254C) and Lsp1 (A254C) formed foci when visualized alone by fluorescence microscopy (not depicted). Bar, 5  $\mu$ m. (B) Number of continuous stretches of 30- or 32-nm diameter plotted versus (y axis) the length of the corresponding Lsp1 filament (in the absence of the membrane). Most filaments exhibit stretches of both narrow and wide diameter. N represents the number of filaments used. (C) Negative staining and EM of recombinant pil1ΔN. In the absence of its N-terminal segment, the pil1ΔN does not form thick helices anymore, only thin filaments. Bar, 100 nm. (D) Localization of Pil1-GFP in wild-type, *pik1<sup>ts</sup>*, and *stt4<sup>ts</sup>* cells after incubation at the restrictive temperature for 90 min and assessed by deconvolution fluorescence microscopy. (E) Localization of Pil1-GFP in wild-type and *vps34Δ* cells, as assessed by deconvolution fluorescence microscopy. (D and E). Bars, 5  $\mu$ m. (F) Sjl1, encoding the PI(4,5)P<sub>2</sub> phosphatase, has the most similar genetic signature to PIL1, indicating similar gene function (Aguilar et al., 2010). CC, correlation of correlations.

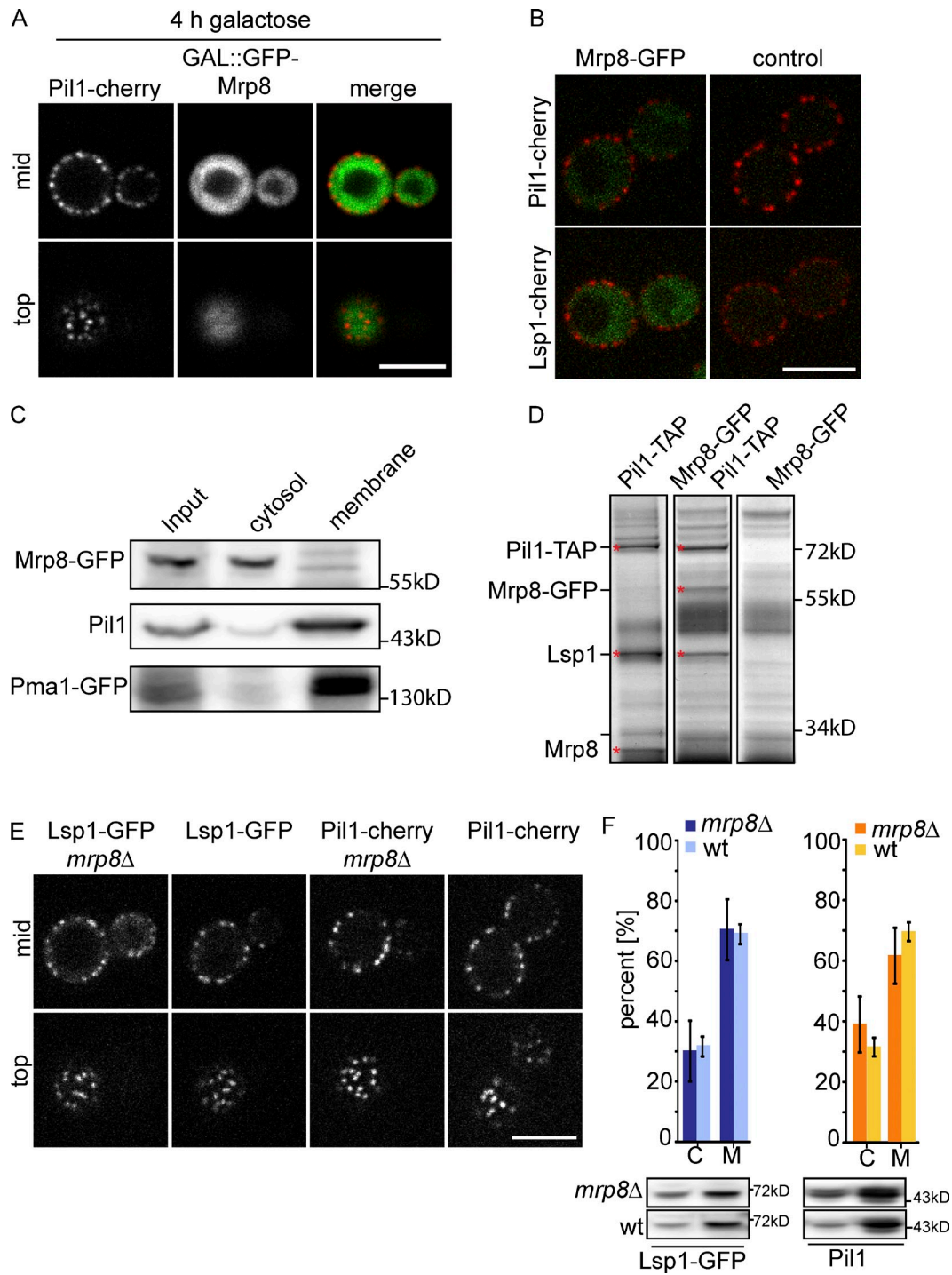


Figure S2. **Mrp8 does not localize in eisosomes and is not required for normal eisosomes.** (A) N-terminally GFP-tagged Mrp8 was expressed from a GAL promoter. Confocal mid and top sections show GFP-Mrp8 localizing in the cytoplasm, distinct from Pil1-cherry-labeled eisosomes. (B) Fluorescence microscopy of C-terminally tagged Mrp8-GFP and expression under its endogenous promoter. Mrp8-GFP localizes in the cytoplasm, distinct from eisosomes marked by Pil1-cherry or Lsp1-cherry. (C) Mrp8-GFP fractionates as a cytosolic protein. Western blot analysis of yeast cell lysate after crude membrane versus cytosol fractionation. The majority of Mrp8 fractionates as a cytoplasmic protein, whereas Pil1 behaves as a membrane protein, similar to Pma1-GFP. (D) Coomassie blue-stained SDS-PAGE of Pil1-TAP immunoprecipitation experiments. Pil1-TAP (Pil1 fused to a tandem affinity purification tag) purifies with Lsp1 as well as with either Mrp8 or Mrp8-GFP. For better visibility, indicated protein bands are marked by red asterisks. (E) *mrp8Δ* deletion has no effect on Lsp1-GFP and Pil1-cherry localization. Confocal mid and top sections are shown. (A, B, and E) Bars, 5  $\mu$ m. (F) Quantification of cytoplasmic (marked as C) versus membrane (marked as M) signal of Lsp1-GFP *mrp8Δ* cells by Western blotting using antibodies recognizing Lsp1-GFP as well as Pil1. Quantification of band intensities shows no significant difference between *mrp8Δ* and control cells. Error bars represent three independent measurements. wt, wild type.

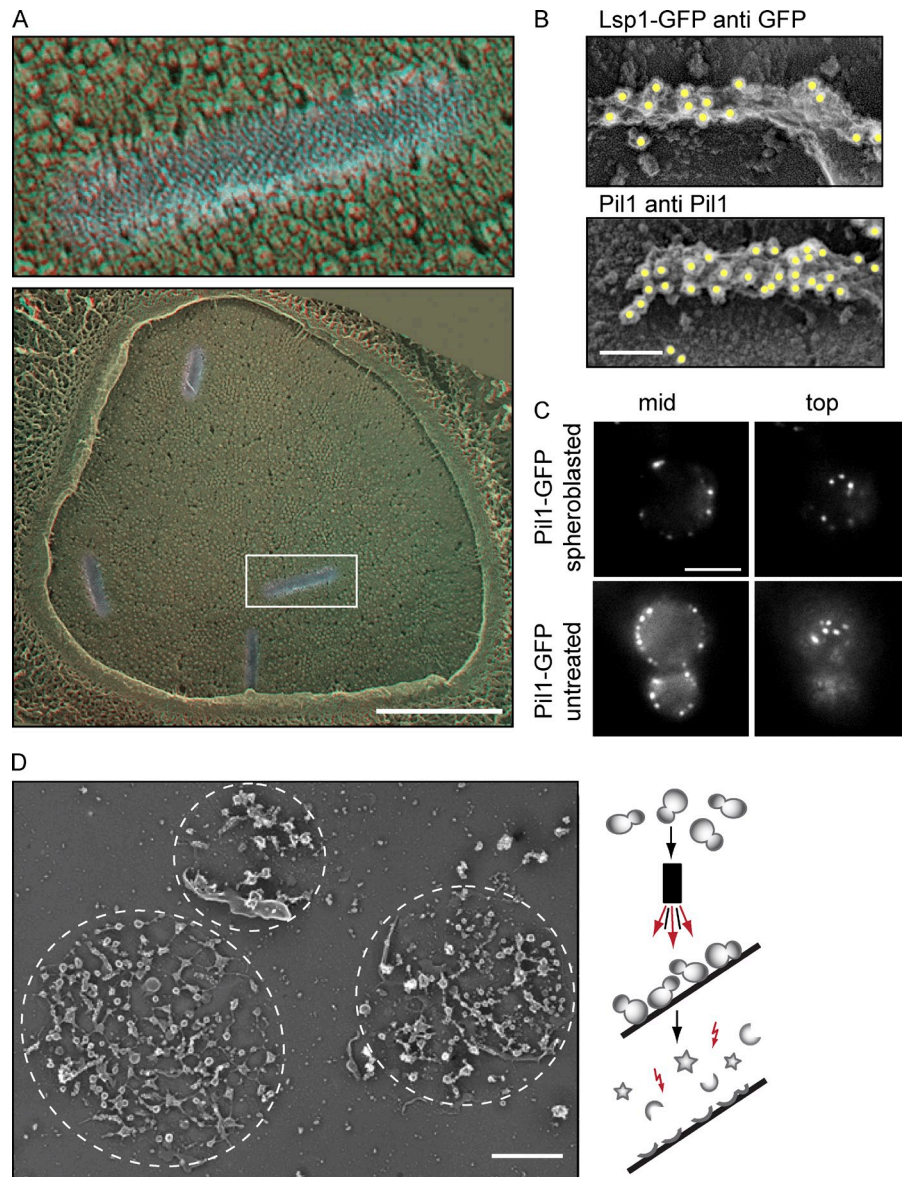
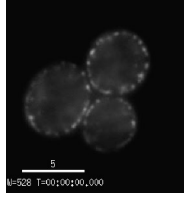
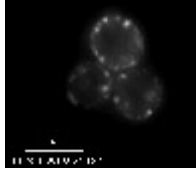


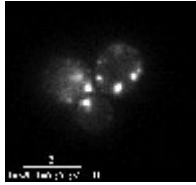
Figure S3. **The yeast plasma membrane exhibits abundant furrows that are PIL1 dependent.** (A) 3D anaglyphs show freeze-fracture views of the yeast plasma membrane (P-face). The membrane exhibits abundant furrows, showing a distinct striation pattern (red cyan 3D glasses are recommended for 3D view). The boxed area is magnified in the top image. Bar, 500 nm. (B) Immunolabeling of plasma membranes of cells expressing Lsp1-GFP using anti-GFP antibodies or wild-type cells using anti Pil1 antibodies. Yellow circles highlight 18-nm gold particles for better visibility. Bar, 100 nm. (C) Fluorescence microscopy of Pil1-GFP in spheroblasted cells treated with zymolyase (top panels) and control cells (bottom panels). Bar, 5 μm. (D) Schematic presentation of workflow for unroofing yeast cells and an overview of plasma membrane fragments generated by this procedure. Magnified selections from such images are shown in Fig. 8. Encircled regions represent areas of plasma membrane fragments generated by this procedure. Bar, 1 μm.



Video 1. **Time-lapse imaging of eisosomes at time point  $t = 0$  min during Mss4 inactivation.** Single-focal plane videos of *mss4<sup>ts</sup>* cells expressing Pil1-GFP at the permissive temperature (24°C). Images were captured using a DeltaVision system equipped with an IX-71 microscope, a 1.35 NA 100x Olympus objective, and a CoolSNAP HQ camera. Frames were taken every 0.5 s. T represents time, whereas W represents the emission wavelength (528 nm) for the FITC filter used in the video. Bar, 5  $\mu$ m.



Video 2. **Time-lapse imaging of eisosomes after 30 min of Mss4 inactivation.** Single-focal plane videos of *mss4<sup>ts</sup>* cells expressing Pil1-GFP after 30 min of a temperature shift to the restrictive temperature (37°C). Images were captured using a DeltaVision system equipped with an IX-71 microscope, a 1.35 NA 100x Olympus objective, and a CoolSNAP HQ camera. Frames were taken every 0.5 s. T represents time, whereas W represents the emission wavelength (528 nm) for the FITC filter used in the video. Bar, 5  $\mu$ m.



Video 3. **Time-lapse imaging of eisosomes after 60 min of Mss4 inactivation.** Single-focal plane videos of *mss4<sup>ts</sup>* cells expressing Pil1-GFP after 60 min of a temperature shift to the restrictive temperature (37°C). Images were captured using a DeltaVision system equipped with an IX-71 microscope, a 1.35 NA 100x Olympus objective, and a CoolSNAP HQ camera. Frames were taken every 0.5 s. T represents time, whereas W represents the emission wavelength (528 nm) for the FITC filter used in the video. Bar, 5  $\mu$ m.

Table S1. **Yeast strains used in this study**

Strain	Genotype	Reference
TWY138	<i>MAT<math>\alpha</math> ura3 trp1 leu2 his3 ade2 can1-100</i>	Walther et al., 2006
TWY1512	<i>MAT<math>\alpha</math> ura3 trp1 leu2 his3 ade2 can1-100 lsp1<math>\Delta</math>::HIS Pil1-GFP::KAN</i>	This study
TWY1952	<i>MAT<math>\alpha</math> ura3 trp1 leu2 his3 ade2 can1-100 lsp1-GFP::HIS pil1<math>\Delta</math>::NAT</i>	This study
SEY6210	<i>MAT<math>\alpha</math> leu2-3, 112 ura3-52 his3-200 trp1-901 lys2-801 suc2-9</i>	Robinson et al., 1988
TWY770	<i>SEY6210; Pil1-GFP::KAN</i>	This study
AAY202	<i>SEY6210; mss4<math>\Delta</math>::HIS3MX6 carrying Ycplacmss4-102 (LEU2 CEN6 mss4-102)</i>	Stefan et al., 2002
TWY764	<i>AAY202; Pil1-GFP::URA</i>	This study
TWY2260	<i>AAY202; Pil1-GFP::URA, Sur7-mars::Nat</i>	This study
TWY2491	<i>MAT<math>\alpha</math> ura3 trp1 leu2 his3 ade2 can1-100 lsp1-GFP::HIS mrp8<math>\Delta</math>::HPH</i>	This study
TWY2495	<i>MAT<math>\alpha</math> ura3 trp1 leu2 his3 ade2 can1-100 Pil1-cherry::HIS mrp8<math>\Delta</math>::HPH</i>	This study
TWY2490	<i>MAT<math>\alpha</math> ura3 trp1 leu2 his3 ade2 can1-100 Pil1-cherry::HIS NAT::GAL::GFP-Mrp8</i>	This study
TWY2489	<i>MAT<math>\alpha</math> ura3 trp1 leu2 his3 ade2 can1-100 Pil1-cherry::HIS Mrp8-GFP::HPH</i>	This study
TWY2492	<i>MAT<math>\alpha</math> ura3 trp1 leu2 his3 ade2 can1-100 Mrp8-GFP::HPH</i>	This study
TWY958	<i>MAT<math>\alpha</math> ura3 trp1 leu2 his3 ade2 can1-100 Pma1-GFP::HIS</i>	Howson et al., 2005
TWY344	<i>MAT<math>\alpha</math> his3_1 leu2_0 met15_0 ura3_0 Pil1-TAP::HIS</i>	Howson et al., 2005
TWY2496	<i>MAT<math>\alpha</math> his3_1 leu2_0 met15_0 ura3_0 Pil1-TAP::HIS Mrp8-GFP::HPH</i>	This study

Underlined text represents standard genetic nomenclature denoting MAT $\alpha$  and MAT $\alpha$  as standard names for mating type loci.

Table S2. **Dataset for helical reconstruction**

Sample	Micrographs	Filaments	Segments
Lsp1	218	2,515	55,500
Lsp1-P1(4,5)P <sub>2</sub>	105	158	4,794
Pil1-P1(4,5)P <sub>2</sub>	123	638	15,303

Table S3. Data collection and reconstruction statistics for helical reconstruction

Dataset	Principal layer line orders	Diameter	Turn	Rise	Symmetry	No. of segments	Resolution
		nm	Degrees	Å			Å
Lsp1							
#1	7, -13	30	-53.1	5.5	C1	34,308	25
#2	8, -13	32	-136.0	5.2	C1	9,210	29
Lsp1-liposome							
#1	9, -13	34	-80.8	4.9	C1	1,135	31
#2	8, -14	33	-47.5	10.4	C2	1,725	n/a
#3	8, -12	32	-49.7	22.0	C4	964	n/a
Pil1-liposome							
#1	7, -15	34	49.4	5.1	C1	3,833	29
#2	8, -14	34	-48.2	10.1	C2	2,696	35
#3	8, -15	36	-46.6	4.8	C1	1,744	35
#4	7, -12	31	152.3	5.6	C1	3,917	n/a

n/a, not applicable.

## References

- Aguilar, P.S., F. Fröhlich, M. Rehman, M. Shales, I. Ulitsky, A. Olivera-Couto, H. Braberg, R. Shamir, P. Walter, M. Mann, et al. 2010. A plasma-membrane E-MAP reveals links of the eisosome with sphingolipid metabolism and endosomal trafficking. *Nat. Struct. Mol. Biol.* 17:901–908. <http://dx.doi.org/10.1038/nsmb.1829>
- Howson, R., W.K. Huh, S. Ghaemmamghami, J.V. Falvo, K. Bower, A. Belle, N. Dephoure, D.D. Wykoff, J.S. Weissman, and E.K. O'Shea. 2005. Construction, verification and experimental use of two epitope-tagged collections of budding yeast strains. *Comp. Funct. Genomics.* 6:2–16. <http://dx.doi.org/10.1002/cfg.449>
- Robinson, J.S., D.J. Klionsky, L.M. Banta, and S.D. Emr. 1988. Protein sorting in *Saccharomyces cerevisiae*: Isolation of mutants defective in the delivery and processing of multiple vacuolar hydrolases. *Mol. Cell. Biol.* 8:4936–4948.
- Stefan, C.J., A. Audhya, and S.D. Emr. 2002. The yeast synaptojanin-like proteins control the cellular distribution of phosphatidylinositol (4,5)-bisphosphate. *Mol. Biol. Cell.* 13:542–557. <http://dx.doi.org/10.1091/mbc.01-10-0476>
- Walther, T.C., J.H. Brickner, P.S. Aguilar, S. Bernales, C. Pantoja, and P. Walter. 2006. Eisosomes mark static sites of endocytosis. *Nature.* 439:998–1003. <http://dx.doi.org/10.1038/nature04472>